International Journal of Thermophysics, Vol. 23, No. 5, September 2002 (© 2002)

High-Temperature Properties of Liquid Boron from Contactless Techniques[1]

F. Millot,[2, 3] J. C. Rifflet,[2] V. Sarou-Kanian,[2] and G. Wille[2]

The density, surface tension, and spectral and total hemispherical emissivities of liquid boron obtained with contactless diagnostics are reported for temperatures between 2360 and 3100 K. It is shown that, contrary to previous expectations, liquid boron is denser than the solid at its melting point. It is also shown that the high total emissivity of 0.36 is not consistent with that of a liquid metal as recently claimed. Finally, good agreement is found with previously reported surface tensions and spectral emissivities of liquid boron.

KEY WORDS: density; emissivity; high temperature; levitation; liquid boron; surface tension.

1. INTRODUCTION

Recent experimental X-ray diffraction by Krishnan et al. [1] and *ab initio* molecular-dynamics simulation by Vast et al. [2] of the microscopic properties of liquid boron have opened questions concerning the basic macroscopic properties of this compound. In particular, the density of liquid boron is a hidden parameter of these two studies. In the work of Krishnan et al. [1] the analysis procedure of the experimental data used the density as a fitting variable giving a liquid density value at melting of approximately 2.07 $g \cdot cm^{-3}$. In the work of Vast et al. [2] a density of $\approx 2\ g \cdot cm^{-3}$ is used. In both cases the densities for liquid boron at the melting point are smaller than the value of 2.17 $g \cdot cm^{-3}$ estimated by Tsagareishvili and Tsagareishvili [3] for the density of solid boron at its melting point.

[1] Paper presented at the Sixth International Workshop on Subsecond Thermophysics, September 26–28, 2001, Leoben, Austria.

[2] CRMHT/CNRS, 1D avenue de la Recherche Scientifique, 45071 Orléans Cedex 2, France.

[3] To whom correspondence should be addressed. E-mail: millot@cnrs-orleans.fr

0195-928X/02/0900-1185/0 © 2002 Plenum Publishing Corporation

Aerodynamic levitation techniques that allow high temperature diagnostics without pollution up to 3200 K has been improved recently in order to get reliable data on liquids [4, 5]. Boron is a good example of the progress that is possible with this experimental technique. The very limited knowledge on liquid boron has led us to extend the density measurement to other macroscopic quantities (surface tension, total emissivity, spectral emissivity), sometimes because it was necessary to understand our observations and sometimes because it was easy to do.

2. EXPERIMENTAL METHODS

We have used aerodynamic levitation to maintain a spherical boron drop about 3 mm in diameter on a gas (argon containing 10% hydrogen) flowing in a "convergent-divergent" steel nozzle as shown on Fig. 1. A CO_2 laser (maximum power of 800 W) with a beam of 1 cm in diameter is used to heat from the top. The laser beam is partially absorbed by the drop and almost completely reflected by the walls of the nozzle. A high temperature

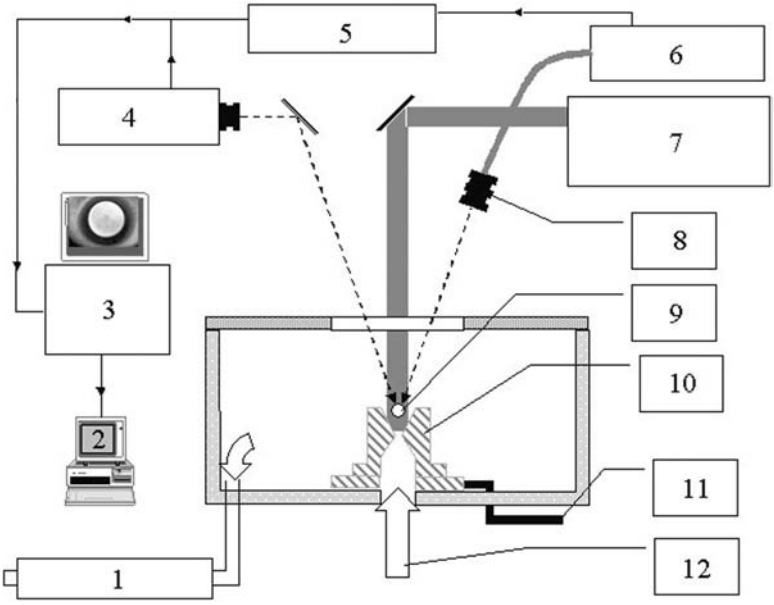

Fig. 1. Experimental setup: (1) oxygen analyzer; (2) image analysis; (3) motion analyzer; (4) high speed camera; (5) multichannel data link; (6) optical pyrometers: (7) CO_2 laser: (8) optical setup; (9) boron drop; (10) nozzle; (11) water cooling; (12) levitation gas.

liquid boron drop is then obtained in a few seconds and the levitation is very stable, the translations of the drop in the nozzle being of the order of a few microns.

The boron drop was originally obtained by melting in the levitation nozzle a pellet that was prepared by axial compression of 99.995% pure amorphous submicron boron. During these processes we noted two possible sources of pollution of the drop:

(a) Boron powder scratches the steel container used for compression.

(b) Formation of a drop from the pellet with the CO_2 laser is a difficult task. Boron sometimes slightly sticks to the steel nozzle, and even if we can separate it apparently without modifying the nozzle surface, we cannot ignore the possibility of iron pollution of the drop.

(c) In order to decide whether pollution is important or not, we have looked at drops after cooling. The EDX analyses revealed no trace of iron inside the drop and slight traces on the very rough surface.

A high-speed digital camera (1000 frames/second) associated with an optical telecentric setup is used to obtain successive frames of the magnified liquid or solid drop. The camera is used for various purposes:

– The 256 grey tones from black to white are used to evaluate the homogeneity of the temperature of the drop.

– In some instances, the high speed of frames (1 ms) allows an evaluation of fast temperature and/or emissivity changes by selecting some pixels of the drop or analyzing all the pixels of the drop.

Image processing of the frames allows transforming them in binary images, which can be easily handled to deduce geometric characteristics such as surface area, diameters, and center of gravity of the two-dimensional image, etc. These data are used to deduce density and surface tension.

Two radiometers operating at $\lambda = 0.55$ and 0.8 μm wavelengths measure light coming from the drop with 10 ms rise time. They are calibrated to obtain temperature measurement T from their output voltage V using the Planck relation:

$$T = \frac{C_2}{\lambda \ln\left(\frac{k+V}{V}\right)} \tag{1}$$

where $C_2 = 14388\ \mu m \cdot K$ and $k = k_0 \varepsilon$ is the product of the normal spectral emissivity ε of the sample with k_0 referring to the optical setup. The calibration consists of determining k_0 and ε. Two experiments are necessary to achieve this, since k_0 and ε are assumed to be temperature independent. k_0 was first obtained from the recalescence of undercooled liquid alumina droplet assuming its emissivity to be 0.93 at the melting point temperature of 2327 K [6].

In the case of boron a reliable melting temperature of 2360 ± 10 K is available from Krishnan et al. [7]. We have then measured the output voltage of the two radiometers during a cooling sequence of the drop. Figure 2 presents a characteristic shape of the free cooling curves. It is difficult from this shape to determine the melting point of boron. We then have used the high-speed camera frames in order to have an image of the drop at the different points of the cooling curve (Fig. 3). We observe that the rise from B to C lasts approximately 15 ms (a very long time compared to the recalescence of undercooled liquids), and it corresponds to a phase change on the surface of the liquid, which starts at various points at different times without simple relations between them. We probably observe the heterogeneous nucleation of solid boron at the melting temperature. This means that the lowest point of the sharp rise at B is related to the emissivity of liquid boron at melting and the highest point at C corresponds to the emissivity of a thin layer of solid boron at the same temperature.

What happens later between C and D is another phenomenon related to the solidification at the melting temperature. We observe an important microstructural change of the surface during the crystallization of the drop. After cooling, its surface observed by SEM looks like a mountain landscape showing occasionally volcanic activity. This change of the surface morphology is happening between points C and D of Fig. 2, explaining the small oscillations of the spinning drop appearing near point D. Another

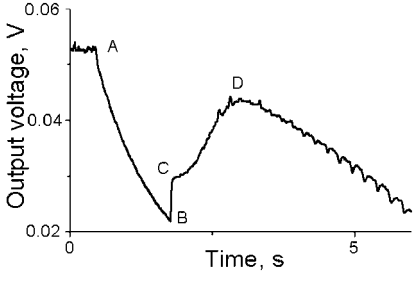

Fig. 2. 0.8 μm pyrometer signal during the free cooling of a liquid boron drop.

Table I. Spectral Emissivity of High Temperature Boron from Fig. 2 Cooling Curve

Pyrometer wavelength (μm)	Spectral emissivity of boron		
	Liquid (B)	Smooth solid (C)	Rough solid (D)
0.55	0.32	0.52	0.66
0.8	0.36	0.50	0.73

characteristic feature is the breaking of the solid drop during cooling, which is indicative of stresses inside it. These observations are clear indications that the volume expansion during solidification is positive or in other words that the density of the liquid is higher than that of the solid.

From the previous discussion we have determined the emissivities of boron at 0.55 and 0.8 μm from 12 different experiments performed at different temperatures (Table I). The standard deviation of these data is 0.02.

The data of Table I is in good agreement with previously reported data obtained at 0.6328 μm wavelength, $\varepsilon_{liq} = 0.31 \pm 0.02$ [1] and $\varepsilon_{sol} = 0.68$ [7].

Emissivities of liquid boron in Table I were used to deduce temperatures from radiometer output voltages.

3. RESULTS

3.1. Density of Liquid Boron

The principle of density measurement has been reported elsewhere [4]. It consists of measuring the size of a liquid drop of known mass obtained with a digital camera and determining the density assuming that the drop has a spherical shape. The mass is measured after cooling.

We have first used a calibrated sphere of alumina to scale the size of pixels. We have made experiments where the camera was looking at drops during heating by the laser and other experiments where drop size was measured during free cooling. Both methods give similar results although the first can be used to obtain the mean density value of 2700 successive frames.

These results obtained at different temperatures are shown in Fig. 4 with a linear fit with a standard deviation of 0.04. Two comments must be made:

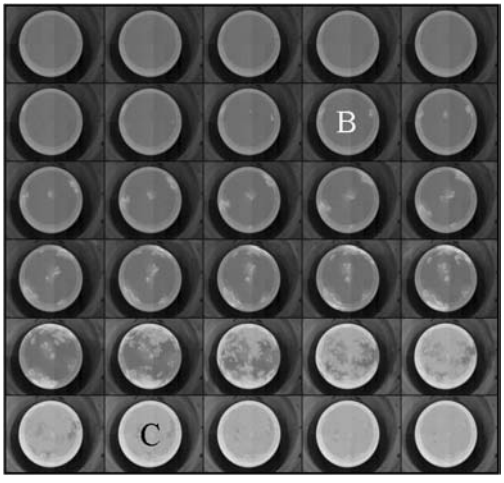

Fig. 3. 1000 Hz frames between B and C points of Fig. 2.

(a) The spherical approximation gives a lower value of the true density by one to two percent. The liquid drop is oblate like earth, the deformation being due to gravity, gas drag, and rotation/precession movement on an approximately vertical axis (rotation frequencies are between 0 and 10 Hz).

(b) Scatter of data may be due to nonspherical object movements inducing changes of the apparent area with frequencies of the order of 1 Hz comparable with the time of the experiment (2 s).

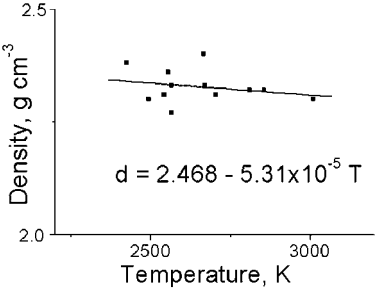

Fig. 4. Density of liquid boron as a function of temperature.

3.2. Surface Tension of Liquid Boron

Vibrations of the $l = 2$ mode of the liquid drop were easily observed. FFTs of characteristic dimensions of the drop showed five peaks characteristic of pseudo-spherical vibration frequencies ν_{2i} of a drop rotating and precessing on an approximately vertical axis [5]. The surface tensions σ shown in Fig. 5 were simply obtained from

$$\sigma = \frac{3\pi m}{40}\left(\sum_{i=-2}^{+2} \nu_i^2\right) \tag{2}$$

Good agreement is obtained with the value of 1060 ± 50 mN·m^{-1} obtained at the melting temperature by Tavadze et al. [8] using the falling drop method on 99.8% pure boron.

3.3. Total Emissivity of Liquid Boron

Cooling curve of the liquid between point A and B of Fig. 2 can be used to determine the ratio of total emissivity ε_T to heat capacity c_p. At temperatures higher than 2000°C, cooling is essentially radiative. The following equation expresses the heat balance equation:

$$mc_p \frac{dT}{dt} + \varepsilon_T \sigma_{SB} S T^4 = 0, \tag{3}$$

where m is the mass of the drop, S is its area, t is the time, and $\sigma_{SB} = 5.67 \times 10^{-8}$ W·m^{-2}·K^{-4} is the Stefan–Boltzmann constant.

Fitting the experimental curve to this expression requires knowledge of the temperature dependence of the emissivity. We have examined two extreme cases:

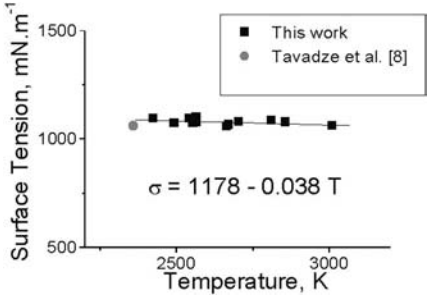

Fig. 5. Surface tension of liquid boron as a function of temperature.

(a) The formula expected if liquid boron is a metal $\varepsilon_T = kT$ [9] where k is a constant. It corresponds to the prediction of Vast et al. [2].

(b) The usual assumption for nonmetallic materials $\varepsilon_T = k$, where k is a constant.

The two procedures have been used on twelve different results obtained with three different pyrometers at 0.4, 0.55, and 0.8 μm wavelengths. The result of the fitting procedure did not allow discrimination between the two hypothetical assumptions. Taking $c_p = 31.75\ \mathrm{J \cdot mol^{-1} \cdot K^{-1}}$ [10] results in values between $\varepsilon_T = 0.35$ and 0.37 at the melting point.

4. DISCUSSION

Little is known about boron properties because it has been recognized for a long time that it is difficult to have it free from pollution. Actually, our data were probably obtained on boron very slightly polluted by iron. Contrary to the previous work by Krishnan et al. [1], we were not able to observe undercooled liquid, indicating that something on the surface of the drop could be used to nucleate boron crystals at the melting temperature.

This problem was perhaps fortunate because it allowed us to measure the emissivities of liquid, smooth, and rough solid boron at the melting point.

Figure 2 for boron looks very much like previously published cooling curves for silicon by Rhim et al. [11, 12]. They observe as we do for boron a first rise in about 30 ms followed by a slow rise up to a plateau. The authors had chosen point C of the curve as being representative of liquid silicon at the melting point. It is really questionable if this is a good choice. More generally speaking, all the studies [11–16] involved with thermophysical properties of boron, silicon and germanium which present a semiconductor-metal transition on melting should be re-examined closely by their authors with respect to temperature calibration. It is quite possible that the temperature proposed in these papers is in excess of the true temperature.

Our data show that the density of liquid boron is higher than that of solid boron. We can estimate the density of solid boron at melting from the work of Tsagareishvili et al. [17] as $d_{sol} = 2.17\ \mathrm{g \cdot cm^{-3}}$ and our work, $d_{liq} = 2.34\ \mathrm{g \cdot cm^{-3}}$ at the same temperature. We then have an approximate 8% contraction on melting instead of the previously accepted dilatation of 9% [3]. The contraction on melting is also substantiated by the similarity of the two cooling curves of silicon and boron and also by the appearance of the surface of the boron drop after cooling.

Another interesting point is that the room temperature density of crystalline boron (2.34 $g \cdot cm^{-3}$) is smaller than that of amorphous boron (2.37$g \cdot cm^{-3}$) [18].

Our results on density may change slightly the conclusion of the study of the structure of liquid boron from X-ray diffraction of Krishnan et al. [1]. As we said in the introduction, density is a parameter of the analysis of the data. We expect mainly a small increase of the coordination number of liquid boron proposed by Krishnan et al. (5.8 ± 1.0) if we adopt our value of 2.34 $g \cdot cm^{-3}$ instead of their value of 2.07 $g \cdot cm^{-3}$.

The total emissivity measurement of our study is probably not very accurate because it is based on an estimated value of the heat capacity of the liquid. In any case we have presented this result because the value of $\varepsilon_{liq} = 0.36$ is much too high to pretend that liquid boron is metallic. If, for example, we apply the Schmidt–Eckert correlation, valid for high-temperature metals [9], we obtain a conductivity of liquid boron at melting of 0.15 $\Omega^{-1} \cdot cm^{-1}$. Recently, two papers have been published coming to the same conclusions with respect to the nonmetallic character of liquid boron:

(a) Glorieux et al. [16] have determined the electrical conductivity σ of liquid boron with a contactless technique. From the value of $\sigma = 960 \pm 50\ \Omega^{-1} \cdot cm^{-1}$ near the melting point it was concluded that liquid boron is not a metal.

(b) Malot et al. [19] have examined the reflectivity of a 10.6 μm laser beam on the surface of solid and liquid boron. They have obtained values of 0.25 for solid and 0.1 for liquid. Again we conclude from the small value of reflectivity of liquid boron that it is not a metal.

The prediction of Vast et al. [2] from molecular dynamics simulation of the metallic character of liquid boron is at variance with optical as well as electrical properties reported in this study and in the literature. It is perhaps the choice of $d_{liq} = 2.0$ $g \cdot cm^{-3}$ in their calculation (instead of 2.34 $g \cdot cm^{-3}$) which is the reason of this discrepancy.

Surface tensions reported in our study show good agreement with the only reported value in the literature [8]. This value was obtained on 99.8% pure boron by a contactless technique, which consists of measuring the weight of drops falling from solid rods of known diameters heated on their extremity. This method is particularly interesting because it is a direct measurement of surface tension. The good agreement of our results with this previous work probably indicates that we have measured a surface tension representative of pure boron. Other arguments may be found in the

fact that the temperature dependence of density and surface tension are similar ($(2\pm3)\times10^{-5}\,K^{-1}$ and $(3\pm1)\times10^{-5}\,K^{-1}$, respectively), a behavior relating a volume to a surface property of pure material [20] .

5. CONCLUSION

New data for the thermophysical properties of liquid boron from melting to 3100 K have been obtained using a contactless technique. The result is that liquid boron is denser than solid boron at melting, which is contrary to previous expectations. The total emissivity value of the liquid (0.36) is not compatible with the prediction for metallic liquids from Monte Carlo simulations.

Cooling curves of the liquid show no undercooling. The spectral emissivities deduced from these curves are in fair agreement with previously published data. The question is raised of a possible misunderstanding of similar cooling curves on liquid boron, silicon and germanium by other authors. Finally, surface tension measurements up to 3100 K confirm the only reported value at the melting point of boron in the literature.

REFERENCES

1. S. Krishnan, S. Ansell, J. J. Felten, K. J. Volin, and D. L. Price, *Phys. Rev. Lett.* **81**:586 (1998).
2. N. Vast, S. Bernard, and G. Zerah, *Phys. Rev. B* **52**:4123 (1995).
3. S. H. Tsagareishvili and G. V. Tsagareishvili, *J. Less Common Metals* **67**:541 (1979).
4. B. Glorieux, F. Millot, J. C. Rifflet, and J. P. Coutures, *Int. J. Thermophys.* **20**:1085 (1999).
5. F. Millot, J. C. Rifflet, G. Wille, V. Sarou-Kanian, and B. Glorieux, *J. Amer. Ceram. Soc.* **85**:187 (2002).
6. F. Millot, B. Glorieux, and J. C. Rifflet, *Prog. Astronautics and Aeronautics* **185**:777 (1999).
7. S. Krishnan, P. Nordine, K. K. R. Weber, and R. A. Schiffman, *High Temp. Sci.* **31**:45 (1992).
8. F. N. Tavadze, I. A. Bairamashvili, D. V. Khantadze, and G. V. Tsagareishvili, *Dokl. Akad. Nauk. SSSR* **150**:544 (1963).
9. Y. S. Touloukian and D. P. DeWitt, *Thermophysical Properties of Matter, The TPRC Data Series* (Plenum, New-York, 1970).
10. M. W. Chase, Jr., C. A. Davies, J. R. Downey, Jr., D. J. Frurip, R. A. MacDonald, and A. N. Syverud, JANAF thermochemical tables, 3rd Ed., *J. Phys Chem. Ref. Data* **14**:177 (1985).
11. W. K. Rhim, S. K. Chung, A. J. Rulison, and R. E. Spjut, *Int. J. Thermophys.* **18**:459 (1997).
12. W. K. Rhim and K. Ohsaka, *J. Crystal Growth* **208**:313 (2000).
13. W. K. Rhim and T. Ishikawa, *Int. J. Thermophys.* **21**:429 (2000).
14. M. Przyborowski, T. Hibiya, M. Eguchi, and I. Egry, *J. Cryst. Growth* **151**:60 (1995).
15. T. Hibiya and S. Nakamura, *Int. J. Thermophys.* **17**:1191 (1996).

16. B. Glorieux, M. L. Saboungi, and J. E. Enderby, *Europhys. Lett.* **56**:81 (2001).
17. G. V. Tsagareishvili, D. SH. Tsagareishvili, and A. G. Khvedelidze, *J. Less Common Met.* **75**:141 (1980).
18. D. R. Lide, ed., *Handbook of Chemistry and Physics*, 79th Ed. (CRC Press, Boca Raton, Florida, 1998).
19. T. Malot, R. Fabbro, D. Grevey, P. Peyre, L. Sabatier, and S. Henry, *Laser Materials Processing (Laser Institute of America, ed.)* **89**:D210–D219 (2000).
20. A. Tegetmeier, A. Cröll, and K. W. Benz, *J. Cryst. Growth* **141**:451 (1994).